




RESEARCH ARTICLE

Crosslinking Super Yellow to produce super OLEDs: Crosslinking with azides enables improved performance

Michael Hengge¹  | Paul Hänsch²  | Daniel Ehjei^{3,4,5} |
Frank S. Benneckendorf^{3,4}  | Jan Freudenberg^{3,4}  | Uwe H. F. Bunz^{3,4,6}  |
Klaus Müllen⁵  | Emil J. W. List-Kratochvil^{1,2}  | Felix Hermerschmidt² 

¹Helmholtz-Zentrum Berlin für Materialien und Energie GmbH, Berlin, Germany

²Humboldt-Universität zu Berlin, Institut für Physik, Institut für Chemie, IRIS Adlershof, Berlin, Germany

³Organisch-Chemisches Institut, Ruprecht-Karls-Universität Heidelberg, Heidelberg, Germany

⁴InnovationLab, Heidelberg, Germany

⁵Max Planck Institute for Polymer Research, Mainz, Germany

⁶Centre for Advanced Materials, Ruprecht-Karls-Universität Heidelberg, Heidelberg, Germany

Correspondence

Felix Hermerschmidt, Humboldt-Universität zu Berlin, Institut für Physik, Institut für Chemie, IRIS Adlershof, Zum Großen Windkanal 2, 12489 Berlin, Germany.

Email: felix.hermerschmidt@hu-berlin.de

Funding information

German Federal Ministry of Education and Research, Grant/Award Number: FKZ 13N13695; Helmholtz-Zentrum Berlin

Abstract

An increasing number of organic light-emitting diodes (OLEDs) is nowadays based on the use of polymers as the emissive material. For this material class in particular, solution-processing of the OLEDs has gained traction in both research and industry. However, in order to access multilayer material systems, orthogonal solvents must be used to prevent dissolution of previously prepared layers. The use of crosslinkers can facilitate this production method by reducing the number of orthogonal solvents needed since insoluble networks are generated. In this work, a novel bisazide crosslinker is employed to insolubilize Super Yellow, a polyphenylene-vinylene emitter. This allows the use of an additional poly[bis(4-phenyl)(2,4,6-trimethylphenyl)amine electron blocking layer (EBL) from the same solvent. Devices including the blocking layer show improved efficacies compared to reference devices without the additional EBL, while also maintaining the emission spectrum. Using the upscalable technique of doctor blading, OLEDs were fabricated which showed a particularly noticeable effect of the blocking layer with a nearly twofold increase in luminance and a 56% increase in current efficacy.

KEYWORDS

crosslinking, multilayer heterojunction, organic light-emitting diode, solution-processing

1 | INTRODUCTION

Since their introduction to the display and lighting markets, organic light-emitting diodes (OLEDs) have been incorporated into a multitude of different appliances such as TVs and smartphone displays.¹ Being thin, flexible, and relatively easy to produce still makes them a topic of high interest in academic as well as industrial research.²

While in general being a fairly simple concept, an organic emitter is sandwiched between conductive electrodes (of which at least one must be transparent); this most simple approach of an OLED exhibits very low efficiencies. Multiple effects are at work here: Charge carriers can face a so-called injection barrier when traveling from the electrodes into the active materials³; carriers can traverse the emission layer (EML) without recombination,

This is an open access article under the terms of the [Creative Commons Attribution](https://creativecommons.org/licenses/by/4.0/) License, which permits use, distribution and reproduction in any medium, provided the original work is properly cited.

© 2022 The Authors. *Journal of Polymer Science* published by Wiley Periodicals LLC.

or the recombination is not confined to the middle of the emission layer, which can lead to quenching of the emission near the electrodes.⁴ These influences can be counteracted by introducing additional layers into the OLED structure.^{1,5} Injection layers for electrons or holes reduce the injection barrier,⁶ transport layers help to overcome charge carrier imbalance, and blocking layers prevent unwanted passage of the charge carriers without recombination.^{7,8}

Using today's most common industrial production method for OLEDs, thermal evaporation, these additional layers can be incorporated without difficulty. Individual layers are successively deposited by thermally vaporizing the base material, which then condenses on top of the previous layer.⁹ However, thermal evaporation has its drawbacks. Not every OLED material evaporates without decomposition, and vacuum deposition techniques typically exclude high molecular weight materials, such as polymers, of which only a few can be evaporated.^{10,11} In these cases, polymer coating is achieved by a combination of thermal depolymerization, evaporation, and deposition of the monomers onto the substrate with concomitant repolymerization.¹² As an alternative technique for these materials, solution-processing is the deposition method of choice.^{9,13} Materials are dissolved in organic solvents and deposited by thin-film forming techniques such as spin coating,^{14,15} blade coating,^{16,17} spray coating,^{18,19} roll-to-roll processing,²⁰ or inkjet-printing.^{21–24} Deposition from solution is challenging since deposited layers can be redissolved upon addition of the next layer. Therefore, care must be taken when choosing the solvents and a so-called orthogonal solvent system (each solvent must not dissolve the previous layer) has to be found.^{25,26} For many molecules and polymers, however, this is a difficult task as several of them have similar solubilities in “standard” organic solvents such as toluene or tetrahydrofuran.

A solution to this problem is the reduction of the contact time of the previously deposited layer with the next solvent or to entirely reduce its solubility (in the best case making it fully insoluble, thereby “fixing” the layer). Several approaches have already been developed for this task. For example, poly(9,9-dioctylfluorene-*alt*-N-[4-sec-butylphenyl]-diphenylamine) (TFB), a material commonly used as a hole-transport and electron-blocking layer, can be thermally stabilized to make it less soluble.^{15,27} This process has also been shown for Super Yellow,²⁸ but literature also indicates that the material degrades under heat.²⁹ For other polymers, so-called crosslinking can be a suitable approach, whereby soluble polymer chains are linked together to form an insoluble polymer network.³⁰

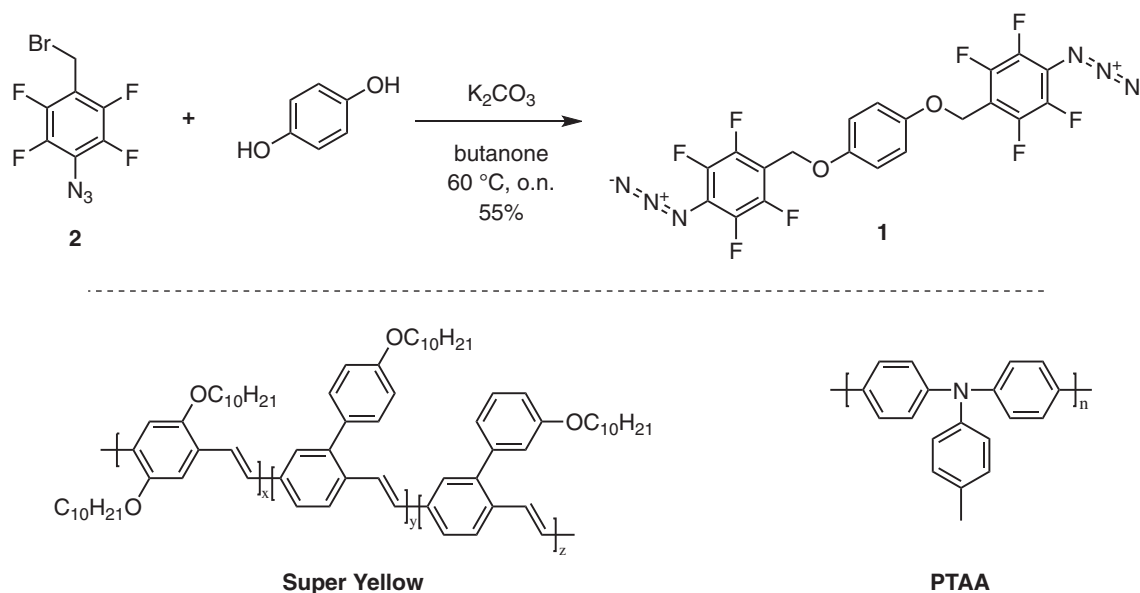
Several types of crosslinking strategies and mechanisms are already well known in literature and will only be portrayed briefly here.^{31–33} Most techniques are based on endowing the polymer side chains with reactive functional groups. Silanes,^{34,35} styrenes,³² acrylates,^{36,37} and oxetanes have been successfully used as crosslinkers.^{13,14} However, all of the aforementioned materials have their own drawbacks. Side products may require additional removal steps and unfavorable crosslinking conditions such as high temperatures or high material selectivity must be considered. While some crosslinkers can be directly activated by light or heat, initiators are occasionally required.³²

A drawback of these crosslinking strategies is that each polymer has to be specifically functionalized and no “off-the-shelf” products can be used. To resolve this issue, reactive molecular crosslinkers have been developed which are used as simple additives. These can target several substituents/functional groups and are therefore (more) universally applicable.

Special care must be taken when specifically crosslinking an OLED's active layer. The insolubilization of molecules or polymers must not interfere with the π -electron system which could lead to a loss of conductivity or emission. For this reason, a commonly applied group of crosslinkers are nitrenes. Due to their high reactivity, nitrenes have to be formed in-situ during the crosslinking process. Azides are suitable precursors liberating singlet nitrenes.^{38–40} Through thermal or photochemical activation, nitrogen is released and the nitrene is generated. Nitrenes have been utilized to photochemically crosslink organic semiconductors without degradation,⁴¹ and have been considered “universal crosslinkers” owing to the fact that they can react with a wide variety of different polymers like polyfluorenes, polystyrenes, or polythiophenes.^{39,41–44}

In this work, we crosslink Super Yellow (SY), a polyphenylene-vinylene (PPV) material, with an easily accessible bisazide additive in ambient conditions. While being one of the most implemented emitter materials in OLED research, SY has seldom been used with crosslinkers before. Jang et al. employed a tetrabranched azide photo-crosslinker to successfully structure SY and produce multilayer OLEDs from solution under inert conditions, targeting small structures for display applications.⁴⁵ Both their azide and our bisazide crosslinker molecules are used as simple additives to an emitter solution and crosslink the polymer already at low concentrations ($\leq 1\%$). Here, we now target scalable production processes, and after crosslinking, the SY emissive layer can be integrated into an inverted OLED device.

An organic electron blocking layer (EBL) poly[bis(4-phenyl)(2,4,6-trimethylphenyl)amine] (PTAA) is added into the OLED architecture to greatly improve light



SCHEME 1 Synthesis of crosslinker **1** via simple two-fold nucleophilic substitution starting from **2** (o.n. = overnight). Shown below are the structural formulas of the super yellow emitter and PTAA.

output and current efficacy. This is enabled by solution processing from toluene solutions (both for the emissive layer as well as the EBL) as a consequence of desolubilization of the emission layer after network formation. Doctor blading as an upscalable manufacturing method was then applied to produce OLEDs with an active area of 0.49 cm². These devices show improved luminance and current efficacy when including the PTAA EBL. All solution processing in this work was done in ambient conditions.

2 | RESULTS AND DISCUSSION

Azide-functionalized crosslinker **1** was synthesized in one step from literature-known 1-azido-4-(bromomethyl)-2,3,5,6-tetrafluorobenzene (**2**)⁴⁶ via nucleophilic substitution with hydroquinone under basic conditions in 55% yield (Scheme 1). Singlet nitrene generation is expected for this crosslinker after application of photochemical or thermal stimuli.^{47–52} The latter is supported by thermal gravimetric analysis: A mass loss of 11.7% is observed with an onset at 140°C and ending at 204°C, being in good agreement with the theoretical reduction of 10.9%, corresponding to a loss of nitrogen (see Figure S1). After thermal annealing, the disappearance of the IR peak attributed to the azides at 2125.17 cm⁻¹ was evident through comparison to a pristine sample of **1** (see Figure S2).

Crosslinking could already be achieved with a mass concentration as low as 1 wt% of crosslinker in the EML solution. The crosslinking reaction itself can be initiated

TABLE 1 Overview of the crosslinking parameters evaluated for super yellow

Duration	8 h	4 h	1 h	
CL concentration (%wt)	5	1	5	1
Remaining thickness (%)	98	94	93	87

Note: Samples of SY were prepared with different weight percentages of crosslinker. After the crosslinking procedure, thin films were washed with toluene to determine the solvent resistivity. Shown are the crosslinking duration (at 140°C), crosslinker concentration, and remaining percentage of the initial SY film thickness after washing with toluene. Long crosslinking durations (≥ 4 h) led to a high percentage of film remaining. However, even 1 h at a low crosslinker concentration of 1 wt% yields sufficiently insolubilized films.

Abbreviation: SY, Super Yellow.

thermally or via light activation. For the SY emitter used here, the prolonged photoactivation needed is not a viable option since the required wavelength of 254 nm would lead to a rapid degradation of the polymer. Thermal activation at 140°C was therefore chosen.

In order to establish the effectiveness of the crosslinking procedure, washing tests were carried out by spin coating pure toluene onto the crosslinked layer. This is to simulate the effect of solution processing an additional layer (from toluene) onto the emitter layer. The film thicknesses were then measured before and after washing. A high remaining percentage of the original film thickness indicates successful crosslinking. In Table 1 an overview of the results for SY is shown. Unsurprisingly, a prolonged thermal treatment time of 8 h leads to a high percentage of remaining film (>90%).

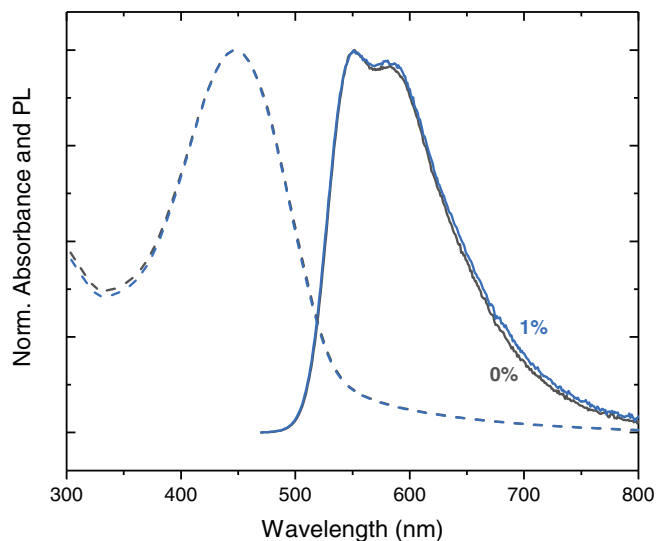


FIGURE 1 Spectral film characterization. Normalized absorbance and normalized photoluminescence (PL) signal of a super yellow film with different percentages of crosslinker added. No shift in absorbance or PL signal peak could be observed at these crosslinker concentrations. Higher percentages of crosslinker were also studied, the graphs are shown in Figure S2.

However, Burns et al. have demonstrated a negative effect of thermal annealing on SY performance.²⁹ Moving to shorter crosslinking times of 4 and 1 h thermal treatment still showed high film retention. As a result, it was concluded that a 1 h interval is sufficient for crosslinking the SY polymer. A low temperature of 140°C, with still more than 80% film retention, was chosen for device fabrication. This low crosslinking temperature also enables the crosslinking process to be compatible with temperature-sensitive substrates such as PET.

To determine if the crosslinker was interfering with the optical properties of the emitter material, absorbance and emission spectra were collected on crosslinked and non-crosslinked thin film blends. Absorption spectra remain unchanged with λ_{max} at 447 nm after the addition of **1** to the SY emitter (see UV-Vis spectra in Figure 1A). This is also the case for the photoluminescence (PL), at least for low percentages of crosslinker. With higher crosslinker percentages ($\geq 5\%$) a broadening of the emission spectrum was observed (see SI, Figure S3). The quantum yield of the emitter only decreases by 0.2% at 1% of added crosslinker. Higher percentages decrease the quantum yield further (see Figure S3). As no blue-shift was observed for absorption or emission, we conclude that as described in literature,⁵³ the mechanism of crosslinking includes CH insertion of nitrenes within the side chains of the emitter, whereas the PPV backbone/chromophore is left intact.

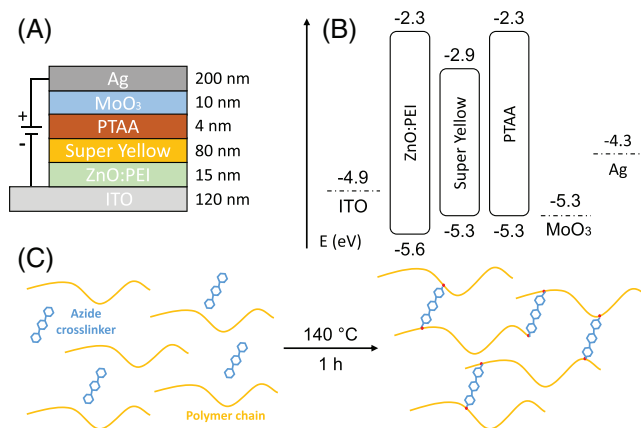


FIGURE 2 Overview of the organic light-emitting diode (OLED) architecture and the crosslinking mechanism. (A) Architecture of the inverted OLED with layer thicknesses. (B) Energy levels of the used materials without interfacial effects.^{54,55} All levels were considered to be aligned at the vacuum level. Dotted lines denote workfunction values. (C) Schematic representation of the crosslinking mechanism. Under the impact of heat, the crosslinker connects the polymer strands within a deposited film, thereby immobilizing the polymer chains and making the film less soluble.

We now fabricated bottom-emitting, inverted OLEDs including the crosslinker and the additional EBL layer consisting of PTAA. In Figure 2A the basic fabrication stack is shown. Figure 2B illustrates the (vacuum-aligned) energy levels of the used materials. The addition of PTAA with its high (compared to SY) lowest unoccupied molecular orbital of -2.3 eV acts as an electron blocking layer and should lower the number of electrons that pass through the device without recombination, thereby increasing device efficiency. As a first step, OLEDs with an active area of 4 mm² were produced. The emissive SY layer was crosslinked in half of the devices. In total for the experimental series, 208 devices with an active area of 0.04 cm² were produced via spin coating, and 86 devices with an active area of 0.49 cm² were fabricated by doctor blading. A PTAA EBL was added to half of the crosslinked and half of the non-crosslinked devices.

To quantify the electrical properties of the OLEDs, current density/voltage/luminance (JVL) curves were measured and are displayed in Figure 3A–C. Current density curves exhibit a faster onset and overall higher values for the reference device when compared to the other devices. Addition of PTAA lowers the current flow significantly. Since this is not the case when including the PTAA in crosslinked devices, it is suggested that this shift is due to partial dissolution of the EML or mixing of the EML with the PTAA. Turn-on voltages (defined as the voltage where the luminance surpasses 1 cd m⁻² for

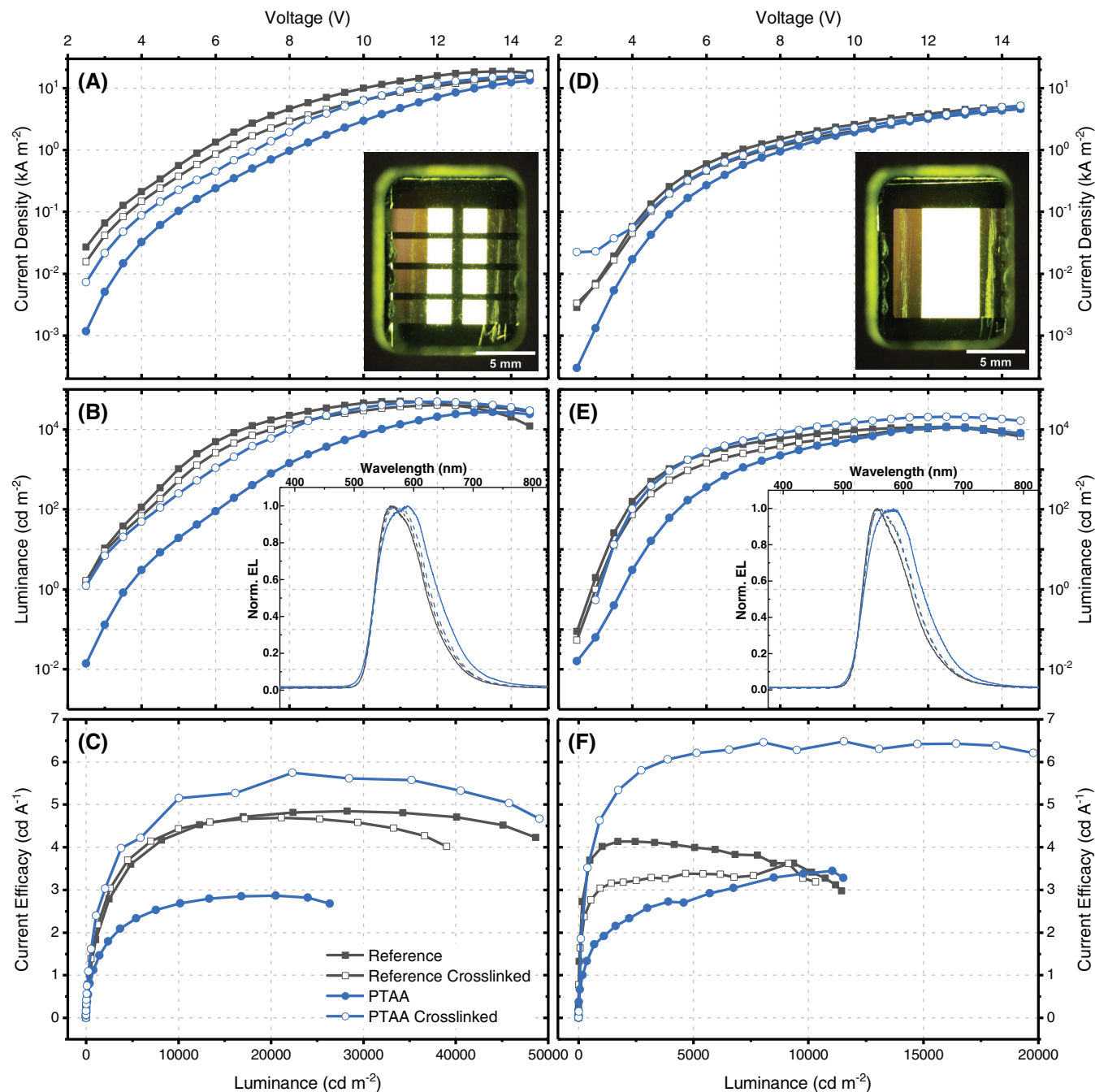


FIGURE 3 Current density/voltage/luminance (JVL) characterizations of spin-coated (left) and doctor-bladed (right) organic light-emitting diode (OLED) devices. The reference is a device with no crosslinker and no poly[bis(4-phenyl)(2,4,6-trimethylphenyl)amine (PTAA). Devices denoted with PTAA have an additional electron blocking layer (EBL) of PTAA added (with and without crosslinking the Super Yellow [SY]). A small loss in performance is visible in the JV curves (A, D) as well as the luminance (B, E) upon addition of the crosslinker. This is compensated by adding the PTAA layer, which greatly improves the overall device efficiency (C, F). For the doctor-bladed devices, this leads to an improvement in performance beyond the reference and a decrease in efficacy roll-off. The insets in A and D show pictures of devices operated at 4 V, while the insets of B and E show normalized EL signals of the devices with and without crosslinker and EBL. PTAA on non-crosslinked SY shifts the EL signal.

the first time) are not affected by the crosslinking process, remaining at an expected V_{on} of approx. 2.5 V for an emitter with a bandgap of 2.4 eV. The addition of PTAA to non-crosslinked devices shifts the whole luminance

curve to higher voltages and thus also the turn-on voltage to 4.0 V. When comparing the luminance results in Figure 3B, crosslinked devices without PTAA lose about 20% of their maximal luminance. The efficiencies of the

TABLE 2 Turn-on voltage (V_{on}), luminance (L), current efficacy (η_c), and CIE1931 coordinates of the fabricated OLEDs

	Type	V_{on} (V)	Peak L (cd m^{-2})	η_c (cd A^{-1}) @ L (cd m^{-2})				CIE1931	
				100	1000	10,000	Peak η_c (cd A^{-1})	x	y
0.04 cm^2	Ref	2.5	49,986	0.54	1.80	4.33	4.85	0.48	0.51
	Ref CL	2.5	40,153	0.48	1.90	4.42	4.69	0.48	0.50
	PTAA	4.0	27,065	0.39	1.23	5.14	2.86	0.51	0.47
	PTAA CL	2.5	49,078	0.72	2.27	2.66	5.75	0.49	0.50
0.49 cm^2	Ref	3.0	11,531	2.12	4.00	3.45	4.14	0.45	0.53
	Ref CL	3.0	11,120	1.75	3.05	3.24	3.62	0.46	0.52
	PTAA	4.5	11,513	0.80	1.88	3.39	3.44	0.48	0.50
	PTAA CL	3.0	20,606	1.79	4.70	6.32	6.48	0.46	0.53

Abbreviations: OLEDs, organic light-emitting diodes; PTAA, poly[bis(4-phenyl)(2,4,6-trimethylphenyl)amine].

reference devices are comparable to OLEDs from the literature that were manufactured under ambient conditions.²¹ When adding PTAA on non-crosslinked SY, the luminance decreases by 46% due to the toluene solution washing away part of the SY layer. The crosslinked SY demonstrates superior stability and is able to return to 98% of the reference luminance. However, due to the lower current density of this material combination, the current efficacy of crosslinked devices incorporating PTAA is greatly improved, as can be seen in Figure 3C. A detailed overview of the device performances can also be found in Table 2.

The insets in Figure 3B are electroluminescence emission spectra of working devices. Between the reference device (SY without crosslinker) and the crosslinked SY device, there is no visible shift in the EL spectra. Both devices have an EL maximum at 565 nm corresponding to CIE1931 coordinates of $(x, y) = (0.48, 0.51)$ for the non-crosslinked reference and $(0.48, 0.50)$ for the reference with crosslinker. When adding PTAA as an EBL to a non-crosslinked device, a redshift in the EL maxima of roughly 25 nm to a maximum of 590 nm is visible, which also leads to slightly shifted CIE coordinates of $(0.51, 0.47)$. In contrast to that, when utilizing the PTAA layer in a device with crosslinked SY, no shift and only a tiny broadening of the spectrum was detectable, leading to CIE coordinates of $(0.49, 0.50)$. It is therefore suggested that the shift is due to interactions between the PTAA and SY or due to the toluene affecting the EML.

So far it could be established that the crosslinking of a Super Yellow emission layer leads to highly solution-stable films. In addition, the inclusion of a PTAA-EBL in OLEDs results in significantly improved performance. Moving to the more scalable device fabrication method of doctor blading, devices with an active area of 0.49 cm^2 were fabricated in the next step. The results are presented in Figure 3D–F and Table 2. While all other devices

exhibit similar behavior at higher voltages above 8 V, the reference device again shows the fastest onset in current density. In terms of luminance, the same trends as for the small area devices are visible. The turn-on voltage for all devices except the non-crosslinked OLED containing PTAA is equal at $V_{\text{on}} = 3$ V. Non-crosslinked OLEDs with PTAA exhibit a turn-on voltage of 4 V. Crosslinked PTAA devices are now able to surpass the reference device in terms of luminance with a peak value of 20,600 cd m^{-2} . As seen in Figure 3F, the current efficacy is vastly improved when adding PTAA in a device containing a crosslinked Super Yellow layer. A maximum efficacy of 6.5 cd A^{-1} could be reached, with a significantly decreased roll-off compared to the reference device. EL spectra (inset in Figure 3E) are again not influenced by the crosslinker with CIE1931 coordinates of $(x, y) = (0.45, 0.53)$ for the non-crosslinked reference, $(0.46, 0.52)$ for the reference with crosslinker and $(0.46, 0.53)$ for crosslinked SY with PTAA. The non-crosslinked PTAA device again shows a slightly shifted spectrum with coordinates of $(0.48, 0.50)$.

3 | CONCLUSION

In conclusion, we have produced crosslinked Super Yellow OLEDs with an additional electron blocking layer of PTAA. The novel bisazide crosslinker allows the PTAA to be solution-processed from the same solvent as the previous layer without dissolution. Devices containing this combination exhibit improved current efficacies in small-area, spin-coated OLEDs with values up to 5.8 cd A^{-1} without altering the emission spectrum. When increasing the active area, the effect of the blocking layer is even more evident with a 78% increase in luminance and 56% increase in efficacy compared to reference devices. Luminance values of 20,000 cd m^{-2} and current efficacies of

up to 6.5 cd A^{-1} with no significant roll-off could be reached for inverted OLEDs. These results are among the highest in the literature for OLEDs fabricated in ambient air conditions and pave the way for further upscaling in the realization of large-area solution-processed OLEDs.

4 | EXPERIMENTAL SECTION

4.1 | Synthesis

See Supporting Information.

4.2 | Solution preparation

The crosslinker and the PDY-132 (Super Yellow, Sigma-Aldrich) light-emitting polymer were dissolved in toluene at concentrations of 5 mg ml^{-1} each and mixed in the desired ratios. Solutions were subsequently stirred at 50°C on a hotplate for several hours. A polyethyleneimine (PEI) solution was made by dissolving PEI (Sigma Aldrich, $M_w = 25,000 \text{ g mol}^{-1}$) in isopropanol at a concentration of 0.4 wt% according to literature.⁵⁶ The zinc oxide (ZnO) nanoparticle solution (Genesink, 1% dispersion in isopropanol, particle size 12 nm) was used as received. PTAA (Ossila, $M_w = 55,000 \text{ g mol}^{-1}$) was dissolved in toluene at a concentration of 1 mg ml^{-1} .

4.3 | Sample preparation

Soda lime glass for thickness measurements, quartz glass for spectral measurements, and glass substrates with pre-patterned indium tin oxide (ITO) (Psiotec Ltd.) for device fabrication were cleaned by wiping them thoroughly with acetone and isopropanol and drying with nitrogen. Sample surfaces were activated by a 5 min O_2 plasma treatment in a Femto plasma system (Diener) at a gas pressure of 0.35 mbar and 500 W of power prior to any solution processing.

4.4 | Crosslinking procedure

Thin films of Super Yellow with or without crosslinker were spin-coated for 60 s at a speed of 2500 rpm with a resulting layer thickness of 80 nm. Crosslinking was performed under vacuum at 140°C for 1 h, if not stated otherwise. The oven was then allowed to slowly cool to room temperature before venting with nitrogen gas.

4.5 | Crosslinker analysis

Fourier transformed infra-red spectra (FTIR) were collected with a Cary 630 FTIR spectrometer (Agilent).

4.6 | Thin-film characterization

UV-Vis absorption spectra were collected with a Perkin Elmer Lambda 950 double-beam spectrometer. Film thickness was determined using a LEXT OLS4100 confocal laser microscope (Olympus) and a DektakXT Stylus Profiler (Bruker). Photoluminescence and photoluminescence quantum yield measurements were performed on an FLS980 fluorescence spectrometer (Edinburgh Instruments Ltd.).

4.7 | Device preparation

OLEDs were fabricated on pre-patterned ITO-coated glass substrates with a 120 nm thick ITO layer. The substrates were cleaned and treated with O_2 plasma as described above. A ZnO:PEI blend (2:1 by volume) was then spin-coated at 2500 rpm and dried for 10 min on a hotplate at 120°C . An emissive SY/crosslinker layer was added (preparation as described above). The PTAA electron blocking layer was doctor-bladed at a speed of 10 mm s^{-1} with a plate temperature of 60°C and subsequently dried at 60°C for 10 min. All solution processing was carried out in ambient conditions. The top electrode consisting of 10 nm of MoO_3 and 200 nm of silver was thermally evaporated under vacuum at a base pressure of 10^{-6} mbar. Two shadow masks were used to obtain devices with active areas of 0.04 and 0.49 cm^2 , respectively. Finally, the devices were encapsulated using glass coverslips and a drop of UV-curable resin (Ossila) which was hardened for 10 min under 365 nm light.

ACKNOWLEDGMENTS

This work was conducted in the framework of the Joint Lab GEN_FAB and was supported by the HySPRINT innovation lab at Helmholtz-Zentrum Berlin. The authors thank Professor N. Koch for granting access to laboratory infrastructure. Financial support by the German Federal Ministry of Education and Research (BMBF) through grant no. FKZ 13N13695 (POESIE) is gratefully acknowledged.


CONFLICT OF INTEREST

The authors declare no conflict of interest.

ORCID

Michael Hengge  <https://orcid.org/0000-0003-2488-5870>

Paul Hänsch  <https://orcid.org/0000-0001-9971-8386>

Jan Freudenberg  <https://orcid.org/0000-0003-0998-693X>

Uwe H. F. Bunz  <https://orcid.org/0000-0002-9369-5387>

Klaus Müllen  <https://orcid.org/0000-0001-6630-8786>

Emil J. W. List-Kratochvil  <https://orcid.org/0000-0001-9206-800X>

Felix Hermerschmidt  <https://orcid.org/0000-0001-8292-4124>

REFERENCES

- [1] B. Geffroy, P. le Roy, C. Prat, *Polym. Int.* **2006**, *55*, 572.
- [2] S.-M. Lee, J. H. Kwon, S. Kwon, K. C. Choi, *IEEE Trans. Electron Devices* **1922**, 2017, 64.
- [3] I. D. Parker, *J. Appl. Phys.* **1994**, *75*, 1656.
- [4] A. L. Burin, M. A. Ratner, *J. Phys. Chem. A* **2000**, *104*, 4704.
- [5] S. Negi, P. Mittal, B. Kumar, *Microsyst. Technol.* **2018**, *24*, 4981.
- [6] S. Stolz, M. Petzoldt, N. Kotadiya, T. Rödlmeier, R. Eckstein, J. Freudenberg, U. H. F. Bunz, U. Lemmer, E. Mankel, M. Hamburger, G. Hernandez-Sosa, *J. Mater. Chem. C* **2016**, *4*, 11150.
- [7] D. D. S. Pereira, P. Data, A. P. Monkman, *Display and Imaging* **2017**, *2*, 323.
- [8] B. R. Kaafarani, T. H. El-Assaad, W. A. Smith, S. M. Ryno, F. Hermerschmidt, J. Lyons, D. Patra, B. Wex, E. J. W. List-Kratochvil, C. Risko, S. Barlow, S. R. Marder, *J. Mater. Chem. C* **2019**, *7*, 5009.
- [9] J. Eccher, W. Zajackowski, G. C. Faria, H. Bock, H. von Seggern, W. Pisula, I. H. Bechtold, *ACS Appl. Mater. Interfaces* **2015**, *7*, 16374.
- [10] S. Palsaniya, H. B. Nemade, A. K. Dasmahapatra, *J. Phys. Chem. C* **2019**, *123*, 27959.
- [11] Y. Ohnishi, R. Kita, K. Tsuchiya, S. Iwamori, *Jpn. J. Appl. Phys.* **2016**, *55*, 02BB04.
- [12] K. P. Griksenko, A. M. Krasovsky, *Chem. Rev.* **2003**, *103*, 3607.
- [13] C. D. Müller, A. Falcou, N. Reckefuss, M. Rojahn, V. Wiederhirn, P. Rudati, H. Frohne, O. Nuyken, H. Becker, K. Meerholz, *Nature* **2003**, *421*, 829.
- [14] M. S. Bayerl, T. Braig, O. Nuyken, D. C. Müller, M. Groß, K. Meerholz, *Macromol. Rapid Commun.* **1999**, *20*, 224.
- [15] M. Auer-Berger, R. Trattnig, T. Qin, R. Schlesinger, M. V. Nardi, G. Ligorio, C. Christodoulou, N. Koch, M. Baumgarten, K. Müllen, E. J. W. List-Kratochvil, *Org. Electron.* **2016**, *35*, 164.
- [16] L. Merklein, M. Mink, D. Kourkoulos, B. Ulber, S. M. Raupp, K. Meerholz, P. Scharfer, W. Schabel, *J. Coat. Technol. Res.* **2019**, *16*, 1643.
- [17] J. da You, S. R. Tseng, H. F. Meng, F. W. Yen, I. F. Lin, S. F. Horng, *Org. Electron.* **2009**, *10*, 1610.
- [18] L. Kinner, E. J. W. List-Kratochvil, T. Dimopoulos, *Nanotechnology* **2020**, *31*, 365303.
- [19] L. Kinner, F. Hermerschmidt, T. Dimopoulos, E. J. W. List-Kratochvil, *Phys. Status Solidi (RRL) – Rapid Res. Lett.* **2020**, *14*, 2000305.
- [20] R. Abbel, I. de Vries, A. Langen, G. Kirchner, H. T'Mannetje, H. Gorter, J. Wilson, P. Groen, *J. Mater. Res.* **2017**, *32*, 2219.
- [21] C. Amruth, M. Z. Szymański, B. Łuszczczyńska, J. Ulański, *Sci. Rep.* **2019**, *9*, 8493.
- [22] M. Hengge, K. Livanov, N. Zamoshchik, F. Hermerschmidt, E. J. W. W. List-Kratochvil, *Flex. Print. Electron.* **2021**, *6*, 015009.
- [23] F. Hermerschmidt, P. Papagiorgis, A. Savva, C. Christodoulou, G. Itskos, S. A. Choulis, *Sol. Energy Mater. Sol. Cells* **2014**, *130*, 474.
- [24] F. Hermerschmidt, S. A. Choulis, E. J. W. List-Kratochvil, *Adv. Mater. Technol.* **2019**, *4*, 1800474.
- [25] S. Sax, N. Rugen-Penkalla, A. Neuhold, S. Schuh, E. Zojer, E. J. W. List, K. Müllen, *Adv. Mater.* **2010**, *22*, 2087.
- [26] R. Trattnig, L. Pevzner, M. Jäger, R. Schlesinger, M. V. Nardi, G. Ligorio, C. Christodoulou, N. Koch, M. Baumgarten, K. Müllen, E. J. W. List, *Adv. Funct. Mater.* **2013**, *23*, 4897.
- [27] J.-S. Kim, R. H. Friend, I. Grizzi, J. H. Burroughes, *Appl. Phys. Lett.* **2005**, *87*, 023506.
- [28] A. Köhnen, M. Irion, M. C. Gather, N. Rehmman, P. Zacharias, K. Meerholz, *J. Mater. Chem.* **2010**, *20*, 3301.
- [29] S. Burns, J. Macleod, T. Trang Do, P. Sonar, S. D. Yambem, *Sci. Rep.* **2017**, *7*, 1.
- [30] M. Auer, L. Pevzner, S. Sax, E. J. W. W. List-Kratochvil, in *Supramolecular Materials for Opto-Electronics* (Ed: N. Koch), Cambridge: Royal Society of Chemistry; **2015**, p. 226.
- [31] J. Freudenberg, D. Jänsch, F. Hinkel, U. H. F. Bunz, *Chem. Rev.* **2018**, *118*, 5598.
- [32] C. A. Zuniga, S. Barlow, S. R. Marder, *Chem. Mater.* **2011**, *23*, 658.
- [33] S. Ho, S. Liu, Y. Chen, F. So, *J. Photonics Energy* **2015**, *5*, 057611.
- [34] W. Li, Q. Wang, J. Cui, H. Chou, S. E. Shaheen, G. E. Jabbour, J. Anderson, P. Lee, B. Kippelen, N. Peyghambarian, N. R. Armstrong, T. J. Marks, *Adv. Mater.* **1999**, *11*, 730.
- [35] H. Yan, P. Lee, N. R. Armstrong, A. Graham, G. A. Evmenenko, P. Dutta, T. J. Marks, *J. Am. Chem. Soc.* **2005**, *127*, 3172.
- [36] A. Bacher, C. H. Erdelen, W. Paulus, H. Ringsdorf, H. W. Schmidt, P. Schuhmacher, *Macromolecules* **1999**, *32*, 4551.
- [37] G. Wu, C. Yang, B. Fan, B. Zhang, X. Chen, Y. Li, *J. Appl. Polym. Sci.* **2006**, *100*, 2336.
- [38] M. Schock, S. Bräse, *Molecules* **2020**, *25*, 1009.
- [39] D. E. Falvey, A. D. Gudmundsdottir, *Nitrenes and Nitrenium Ions*, John Wiley & Sons, Inc., Hoboken, NJ **2013**.
- [40] J. Park, C. Lee, J. Jung, H. Kang, K.-H. H. Kim, B. Ma, B. J. Kim, *Adv. Funct. Mater.* **2014**, *24*, 7588.
- [41] R.-Q. Q. Png, P.-J. J. Chia, J.-C. C. Tang, B. Liu, S. Sivaramakrishnan, M. Zhou, S.-H. H. Khong, H. S. O. O. Chan, J. H. Burroughes, L.-L. L. Chua, R. H. Friend, P. K. H. H. Ho, *Nat. Mater.* **2010**, *9*, 152.
- [42] N. Koch Ed., *Supramolecular Materials for Opto-Electronics*, Royal Society Of Chemistry, Cambridge **2014**.
- [43] K. Kim, S. Shin, S. H. Kim, J. Lee, T. K. An, *Appl. Surf. Sci.* **2019**, *479*, 280.
- [44] K. A. Murray, A. B. Holmes, S. C. Moratti, G. Rumbles, *J. Mater. Chem.* **1999**, *9*, 2109.
- [45] W. Jang, M. Lee, H. Kweon, H. W. Park, J. Yang, S. Kim, H. Jo, C. Lee, J. H. Cho, K. Kwak, D. H. Kim, B. S. Kim, M. S. Kang, *ACS Photon.* **2021**, *8*, 2519.
- [46] K. Strömgaard, D. R. Saito, H. Shindou, S. Ishii, T. Shimizu, K. Nakanishi, *J. Med. Chem.* **2002**, *45*, 4038.
- [47] I. O. Huyal, U. Koldemir, T. Ozel, H. V. Demir, D. Tuncel, *J. Mater. Chem.* **2008**, *18*, 3568.

- [48] C. J. Mueller, T. Klein, E. Gann, C. R. McNeill, M. Thelakkat, *Macromolecules* **2016**, *49*, 3749.
- [49] C. Y. Nam, Y. Qin, Y. S. Park, H. Hlaing, X. Lu, B. M. Ocko, C. T. Black, R. B. Grubbs, *Macromolecules* **2012**, *45*, 2338.
- [50] H. J. Kim, A.-R. Han, C.-H. Cho, H. Kang, H.-H. Cho, M. Y. Lee, J. M. J. Fréchet, J. H. Oh, B. J. Kim, *Chem. Mater.* **2012**, *24*, 215.
- [51] J. M. Spruell, M. Wolffs, F. A. Leibfarth, B. C. Stahl, J. Heo, L. A. Connal, J. Hu, C. J. Hawker, *J. Am. Chem. Soc.* **2011**, *133*, 16698.
- [52] K. A. Murray, A. B. Holmes, S. C. Moratti, R. H. Friend, *Synth. Met.* **1996**, *76*, 161.
- [53] R. E. Banks, G. R. Sparkes, *J. Chem. Soc., Perkin Trans.* **1972**, *1*, 2964.
- [54] L. Kinner, T. Dimopoulos, G. Ligorio, E. J. W. W. List-Kratochvil, F. Hermerschmidt, *RSC Adv.* **2021**, *11*, 17324.
- [55] J. H. Noh, S. H. Im, J. H. Heo, T. N. Mandal, S. il Seok, *Nano Lett.* **2013**, *13*, 1764.
- [56] Y. Zhou, C. Fuentes-Hernandez, J. Shim, J. Meyer, A. J. Giordano, H. Li, P. Winget, T. Papadopoulos, H. Cheun, J. Kim, M. Fenoll, A. Dindar, W. Haske, E. Najafabadi, T. M. Khan, H. Sojoudi, S. Barlow, S. Graham, J. L. Brédas, S. R. Marder, A. Kahn, B. Kippelen, *Science* **1979**, *2012*(336), 327.

SUPPORTING INFORMATION

Additional supporting information may be found in the online version of the article at the publisher's website.

How to cite this article: M. Hengge, P. Hänsch, D. Ehjeij, F. S. Benneckendorf, J. Freudenberg, U. H. F. Bunz, K. Müllen, E. J. W. List-Kratochvil, F. Hermerschmidt, *J. Polym. Sci.* **2022**, *1*. <https://doi.org/10.1002/pol.20220120>